Available online at www.sciencedirect.com
SCIENCE DIRECT®
Journal of Molecular Catalysis A: Chemical 217 (2004) 165–174
JOURNAL OF MOLECULAR CATALYSIS A: CHEMICAL
www.elsevier.com/locate/molcata

Side-chain oxidation of ethylbenzene with *tert*-butylhydroperoxide over mesoporous Mn-MCM-41 molecular sieves

S. Vetrivel, A. Pandurangan*

Department of Chemistry, Anna University, Chennai 600025, India

Received 5 November 2003; received in revised form 20 February 2004; accepted 16 March 2004

Abstract

Mesoporous Mn-MCM-41 (Si/Mn = 29, 56, 73 and 104) materials were synthesized by hydrothermal process. Their structures were characterized by X-ray diffraction (XRD). Surface area, pore size and wall thickness were calculated from BET equation and BJH method using nitrogen sorption technique. The thermal property of the as-synthesized materials was studied using thermogravimetric-differential thermal analysis (TG-DTA). Diffuse reflectance UV-Vis spectroscopy confirmed presence of manganese ion in the framework position of the MCM-41. Mn(II) species with a well-resolved singlet, centered at $g = 2.007$, was assigned to have distorted tetrahedral symmetry. The oxidation of ethylbenzene has been carried out over Mn-MCM-41 (Si/Mn = 29, 56, 73 and 104) using *t*-butylhydroperoxide as oxidant at 333–353 K. Mn-MCM-41 (29) was more active than other catalyst, and it retained activity for three cycles of operation. The major products were α-phenylethanol and acetophenone. Benzaldehyde and phenyl acetaldehyde were also observed in minor quantity. The difference in the product selectivity was explained based on the reaction intermediates.

Keywords: MCM-41; Oxidation with TBHP; Ethylbenzene; Acetophenone; α-Phenylethanol

1. Introduction

Side-chain oxidation of alkyl aromatics using cleaner peroxide oxidants catalyzed by heterogeneous catalysts still attracts interests. Classical synthetic laboratory procedures preferably use stoichiometric oxidants such as permanganate and dichromate which are hazardous [1]. Hence, there has been an interest to develop ecofriendly catalysts for the oxidation of alkylaromatics. The oxidation of many organic substrates using H_2O_2 as oxidant over Ti^{4+} analogues of ZSM-5 (TS-1) and ZSM-11 (TS-2) has been well-documented [2–4]. Titanium substituted silicates have been thought to catalyze ring hydroxylation of arenes with H_2O_2, but vanadium [5–12], tin [9–13] and chromium [14–16] substitution into a variety of zeolites and aluminophosphate molecular sieves has led to favored oxidation at the side-chain. The presence of molecular oxygen or single oxygen atom donors such as *tert*-butylhydroperoxide for the oxidation of alkanes to alcohols and ketones are shown to be important [17–20]. Chromium substituted aluminophasphate catalysts are found to favor the formation of ketones from alkyl arenes with TBHP as an oxidant [16]. Manganese analogues of these systems have also been shown to catalyze oxidation of alkanes using TBHP [21–25]. Manganese anchored on silicious MCM-41 at a very high coverage was shown to have high activity for propene oxidation [26,27]. Raja and Thomas [28] reported selective oxidation of dodecane preferentially at C_1 and C_2 carbon over microporous aluminophosphate, ALPO-18. Cyclohexane [29] and alkanes [30] were also oxidized on Mn-MCM-41. Based on these reports, in the present study, we utilized manganese containing MCM-41 molecular sieves as catalysts in the oxidation of ethylbenzene using *t*-butylhydroperoxide as oxidant in liquid phase. The main aim was to understand the course of the reaction, which predominantly occurs through the activation of the primary or the secondary carbon atom of the ethyl substituent without aromatic ring hydroxylation.

* Corresponding author. Tel.: +91-44-22203158; fax: +91-44-2220660.
E-mail address: pandurangan_a@yahoo.com (A. Pandurangan).

1381-1169/$ – see front matter © 2004 Elsevier B.V. All rights reserved.
doi:10.1016/j.molcata.2004.03.022

2. Experimental

2.1. Synthesis of Mn-MCM-41

Manganese incorporated MCM-41 with Si/Mn = 29 was hydrothermally synthesized. In a typical synthesis, 12.2 g (1 mol) sodium metasilicate (44–47% SiO_2) dissolved in 50 g of deionized water was mixed with 0.9 g (0.04 mol) of manganese acetate (dissolved in 10 g of deionized water) solution. This mixture was stirred for 30 min at a speed of approximately 250 rpm and 40 ml of 2N sulfuric acid was added with continuous stirring for another 30 min at a speed of 250 rpm until gel formation. Further 7.2 g (0.2 mol) of cetyltrimethylammonium bromide (CTAB) was added drop by drop (30 ml/h) through the dual syringe pump till the gel transformed into suspension. The molar composition of the resultant mixture was SiO_2: 0.2 CTAB: $X MnO_2$: 0.89 H_2SO_4: 120 H_2O (X varies with the Si/Mn ratio). The suspension was transferred into Teflon-lined steel autoclave and placed in a hot air oven maintained at 165 °C for 48 h. After cooling to room temperature, the material was recovered by filtration, washed with deionized water and ethanol, and finally calcined in flowing air at 550 °C for 6 h.

The catalysts, Mn-MCM–41 with Si/Mn = 56, 73 and 104, were also synthesized in a similar manner, wherein, only the ratio of manganese acetate was adjusted appropriately.

2.2. Physicochemical characterization

The manganese content in Mn-MCM-41 was determined using ICP-AES with Allied Analytical ICAP 9000. The crystalline phase identification and phase purity determination of the calcined samples of Mn-MCM-41 were carried out by X-ray diffraction (XRD) (Scintag 2000 Diffractometer) using nickel filtered, Cu Kα radiation (λ = 1.5406 Å).

The surface area and pore properties of calcined Mn-MCM-41 materials were analyzed using Nova-1000 (QUAN-TACHROME, Version 5.01) sorptometer. Before analysis, the calcined and hydrothermally treated materials were dried at 130 °C and evacuated overnight in flowing argon at a flow rate of 60 ml min^{-1}. Surface area, pore size and wall thickness were obtained from these isotherms using the conventional BET and BJH equations. IR spectra of the samples were recorded with a Nicolet Impact 410 FT-IR spectrometer as KBr pellet (0.005 g sample with 0.1 g KBr) scan number 36, resolution 2 cm^{-1}. The data were treated with OMNIC Software.

Thermogravimetric-differential thermal analysis (TG-DTA) was carried out in a Rheometric scientific (STA 15 H^+) thermo balance. 10–15 mg of as-synthesized Mn-MCM-41 was loaded, and airflow was kept at 50 ml min^{-1}. The rate of heating was 20 °C min^{-1} and the final temperature was 1000 °C. Diffuse reflectance (DR) spectra were recorded between 350 and 2000 nm on a Shimadzu UV-240 spectrometer using $BaSO_4$ as a reference.

X-band (9 GHz) ESR spectra were recorded for calcined materials at liquid nitrogen temperature on a Varian E112 Spectrometer. The relative ESR intensities were calculated by double integration of the recorded signal. The size and morphology of Mn-MCM-41 (29) and Mn-MCM-41 (73) samples were recorded using a JEOL 640 scanning electron microscope (SEM) operating at an accelerating voltage of 10 kV. Samples were mounted using a conductive carbon double-sided sticky tape. The samples were sputtered with gold (ca. 10 nm) to reduce the effect of charging.

2.3. Catalytic oxidation reactions

The oxidation of ethylbenzene was carried out in a RB flask (50 ml capacity) fitted with a condenser, a thermometer and magnetic stirrer. The flask was heated on a temperature-controlled oil bath. The catalyst (0.3 g) was added onto a mixture of ethylbenzene and *t*-butylhydroperoxide (various molar ratio), at the reaction temperatures, viz. 333 and 353 K, for different reaction times (h). The total duration of each run was 24 h. The reaction mixture was withdrawn at regular intervals, centrifugated to remove the catalyst and analyzed by gas chromatography (HP 5890 series II) using a flame-ionization detector and a 50 m × 0.2 mm PONA column (Supelco). The products were identified by GC–MS (Shimadzu) wherever required.

3. Results and discussion

3.1. ICP-AES analysis

The manganese content in Mn-MCM-41 was recorded using ICP-AES with allied analytical ICAP 9000. The results of Si/Mn ratios of the materials are given in Table 1.

3.2. XRD

The powder X-ray diffraction patterns of calcined Mn-MCM-41 (Si/Mn = 29, 56, 73 and 104) material are depicted in Fig. 1. Owing to the long-range order of the mesopores, they show diffractions in the 2θ range of; 2° (1 0 0), broad peaks near 2θ = 3.53° (1 1 0) and 3.83° (2 0 0). Similar XRD patterns were previously reported for Mn-MCM-41 materials with hexagonal structure [31]. Physicochemical properties of these mesoporous materials are summarized in the Table 1. The XRD patterns of calcined Mn-MCM-41 were similar to those of the as-synthesized materials although they showed a reduction in the pore size. The hexagonal unit-cell parameter (a_o) was calculated using d_{100}, which was obtained from Bragg's equation ($2d \sin\theta = n\lambda$, where λ = 1.5406 Å for the Cu Kα line). The value of a_o was equal to the internal pore diameter plus pore wall thickness.

Table 1
Elemental analysis and physicochemical characterization of Mn-MCM-41 materials

Samples	Si/Mn	ICP	Calcined (Å)		BET surface area ($m^2\,g^{-1}$)	Pore size (Å)	Wall thickness (Å)
			d-spacing value	Unit-cell parameter			
Mn-MCM-41 (29)	25	29	44.185	51.021	994	28.6	29.5
Mn-MCM-41 (56)	50	56	44.055	50.870	–	–	–
Mn-MCM-41 (73)	75	73	44.068	50.885	–	–	–
Mn-MCM-41 (104)	100	104	44.273	51.122	1067	30.2	17.0

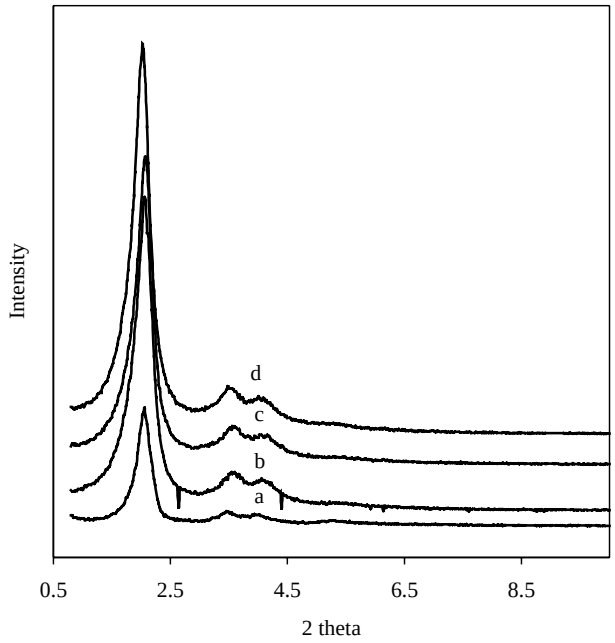

Fig. 1. XRD of: (a) calcined Mn-MCM-41 (29); (b) Mn-MCM-41 (56); (c) Mn-MCM-41 (73); and (d) Mn-MCM-41 (104).

3.3. Adsorption isotherm of nitrogen

Fig. 2 shows the isotherm of nitrogen adsorption of the calcined Mn-MCM-41 (29) and Mn-MCM-41 (104), measured at liquid nitrogen temperature (77 K). All the samples exhibit type (IV) isotherm, characteristic of mesoporous materials with regularly sized pores. Monolayer adsorption on the walls of the mesopores is responsible for the uptake of nitrogen at low relative pressures ($p/p_o < 0.3$). Absence of micropores in the samples was confirmed by *t*-plots. For p/p_o between 0.3 and 0.4, a sharp inflection in the isotherms could be observed, indicating capillary condensation within uniformly sized mesopores. The adsorption and desorption branches matched very well within this range. The pore size distribution, BET surface areas, and the cumulative BJH desorption pore volumes are presented in Table 1. It can be seen that, the pore size of Mn-MCM-41 (29) is higher than that of others due to the presence of textural mesoporosity.

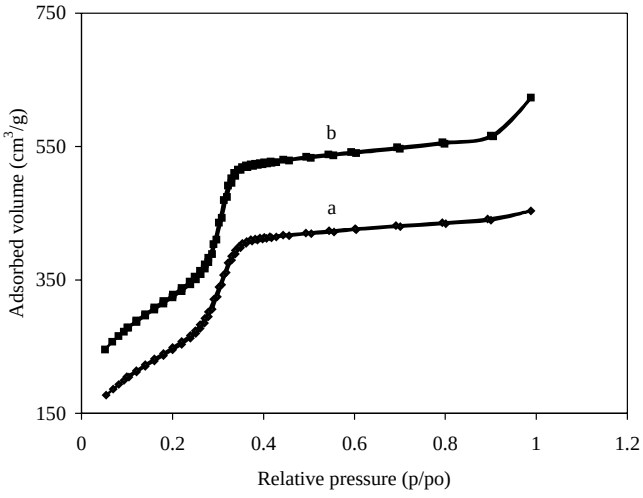

Fig. 2. N_2 adsorption isotherm of: (a) calcined Mn-MCM-41 (29); (b) Mn-MCM-41 (104).

3.4. FT-IR spectroscopy

The framework vibrations of Mn-MCM-41 were analyzed by FT-IR spectra. The FT-IR spectra of all the catalysts are presented in Fig. 3. The as-synthesized sample exhibits absorption bands at 2921 and 2851 cm^{-1} corresponding to symmetric C–H and asymmetric CH_2 vibrations of the surfactant molecules. The broad band around 3500 cm^{-1} may be attributed to surface silanols and adsorbed water molecules, whose deformational vibrations cause the absorption bands between 1623 and 1640 cm^{-1} [32]. The peak between 960 and 970 cm^{-1} is assigned to the incorporation of metal into the framework. Actually this band is assigned to a stretching vibration of Si–O–Mn linkage was observed [33]. The absorption bands at 1057 and 1223 cm^{-1} are due to asymmetric stretching vibration of Si–O–Si bridge. The disappearance of peaks at 2851 and 2921 cm^{-1} in the calcined materials confirms complete loss of template.

3.5. TGA-DTA

Thermogravimetric analysis of as-synthesized Mn-MCM-41 (29), Mn-MCM-41 (56), Mn-MCM-41 (73) and Mn-MCM-41 (104) have shown distinct weight losses that depend, in part, on framework composition (Table 2). Representative thermograms are given in Fig. 4. The TGA patterns have at least three distinct stages of weight loss. A weight loss due to desorption of water amounting to 4.14, 4.51, 4.25 and 5.80% was observed between room

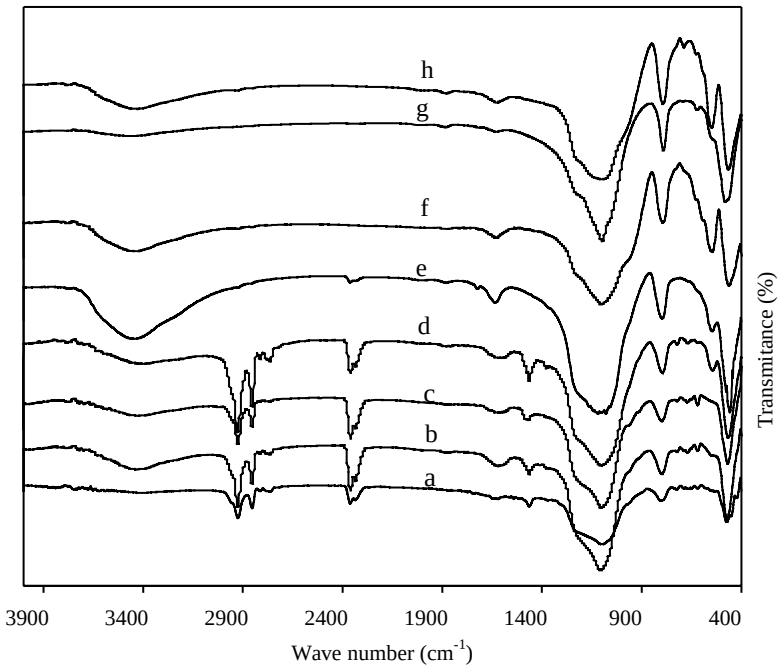

Fig. 3. FT-IR spectra of: (a) as-synthesized Mn-MCM-41 (29); (b) Mn-MCM-41 (56); (c) Mn-MCM-41 (73); (d) Mn-MCM-41 (104); (e) calcined Mn-MCM-41 (29); (f) Mn-MCM-41 (56); (g) Mn-MCM-41 (73); and (h) Mn-MCM-41 (104).

temperature and 150 °C. The stage between 150 and 350 °C corresponding to a weight loss of 22.45, 23.28, 16.02 and 20.71% can be ascribed to the decomposition of surfactant species. The weight loss of 6.06, 6.14, 7.03 and 9.13% from 350 to 650 °C can be assigned to coke calcination and loss of silanol groups.

The DTA curves are shown in the Fig. 4. All the curves in the broad exotherm between 200 and 500 °C coincide with the weight loss in the TGA trace between 200 and 500 °C. Hence, it is ascribed to loss of oxidative decomposition of template. Above 500 °C, there is neither exothermic nor endothermic peak illustrating the materials are stable up to 1000 °C.

3.6. DRS analysis

The co-ordination environment of Mn in Mn-MCM-41 was analyzed by DRS, and Fig. 5 shows the DR spectra of Mn-MCM-41 (Si/Mn = 29 and 73). An intense band centered at ca. 800 nm indicates Mn(II) in tetrahedral coordination in the framework. Generally, these bands are due to

Table 2
Thermogravimetric results (in air) for the Mn-MCM-41 materials

Samples	Weight loss (wt.%)			
	Total	50–150 °C	150–350 °C	350–550 °C
Mn-MCM-41 (29)	32.65	4.14	22.45	6.06
Mn-MCM-41 (56)	34.20	4.51	23.28	6.41
Mn-MCM-41 (73)	27.30	4.25	16.02	7.03
Mn-MCM-41 (104)	35.64	5.80	20.71	9.13

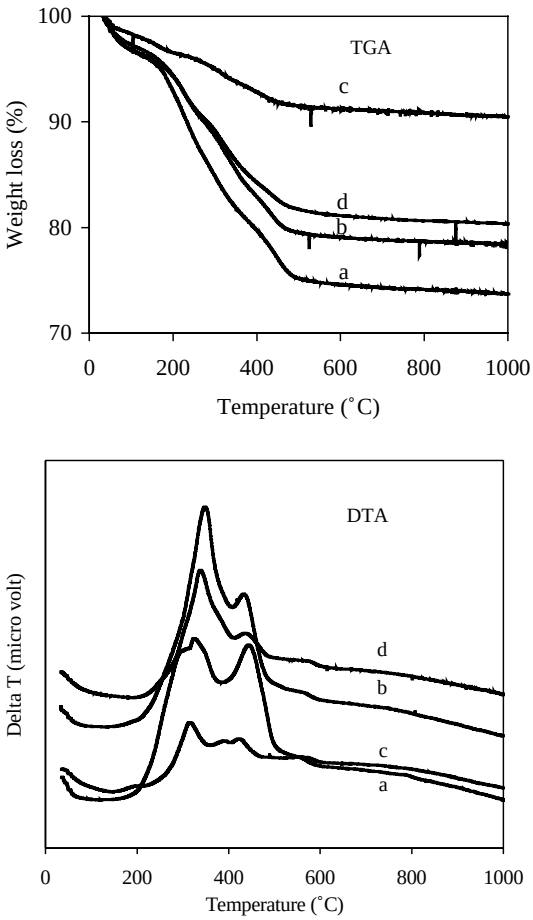

Fig. 4. TG-DTA curve of: (a) as-synthesized Mn-MCM-41 (29); (b) Mn-MCM-41 (56); (c) Mn-MCM-41 (73); and (d) Mn-MCM-41 (104).

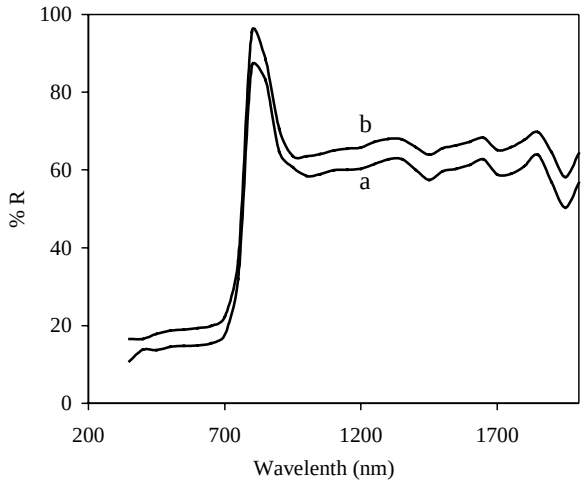

Fig. 5. DR UV-Vis spectra of calcined: (a) Mn-MCM-41 (29); and (b) Mn-MCM-41 (73).

ligand-to-metal charge transfer involving isolated transition metal sites [34].

3.7. ESR spectroscopy

Fig. 6 shows the X-band ESR spectra of calcined Mn-MCM-41 (Si/Mn = 29 and 73) taken at liquid nitrogen temperature. The ESR spectra due to both Mn-MCM-41 (29 and 73) display five signals characteristics of Mn(II) (3d5) species. Mn(III) species which would have been formed during synthesis, is observed to be reduced to Mn(II) during calcination. In the as-synthesized Mn-containing aluminophosphate molecular sieves, synthesized under acidic condition, similar spectra has been reported [35]. The Mn^{2+} substituted MCM-41 molecular sieves show a broad ESR signal with a *g* value of 2.007 (both samples). The broad peaks of the hyperfine signals indicate the strong interaction of Mn^{2+} with their environment in the tetrahedral framework.

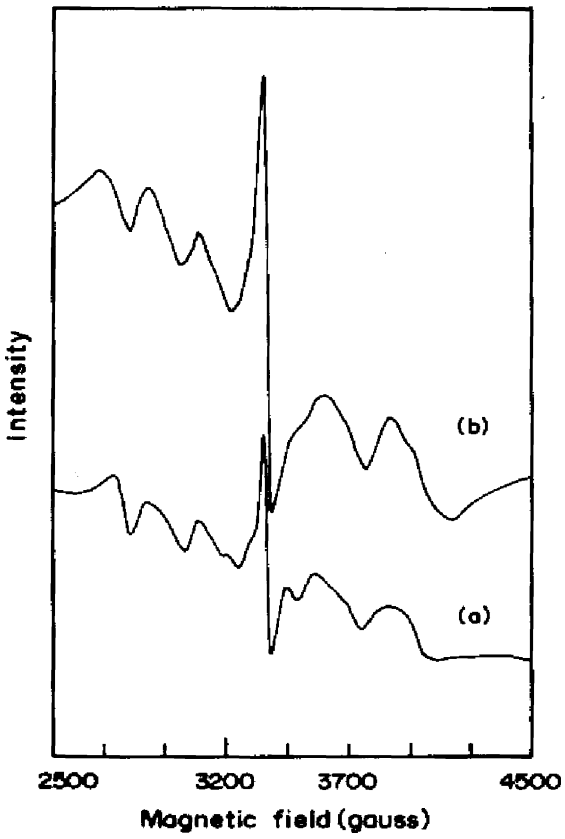

Fig. 6. ESR spectra of calcined: (a) Mn-MCM-41 (29); and (b) Mn-MCM-41 (73).

3.8. Scanning electron microscopy

The morphology and the long-range order of Mn-MCM-41 (29) and Mn-MCM-41 (73) were investigated by scanning electron microscopy. The SEM pictures of these catalysts are presented in Fig. 7a and b. It can be seen that, irrespective of the loading of manganese, the solids have the same morphology corresponding to aggregates without regular shapes, which are in agreement with previous reports [36] for metal incorporated materials. The pictures also show the orderly growth of pure hexagonal phase with well-defined sites.

3.9. Oxidation of ethylbenzene over Mn-MCM-41

The oxidation of ethylbenzene with *t*-butylhydroperoxide over Mn-MCM-41 (Si/Mn = 29, 56, 73 and 104) molecular sieves has been examined at 333 K with the feed ratios of EB: TBHP; 1:1 and 1:3. The results obtained are presented in Table 3. Mn-MCM-41 (29) displays more conversion at the feed ratio of EB: TBHP; 1:3 than 1:1, due to the presence of excess *tert*-butylhydroperoxide coordinated with manganese. At both the feed ratios, the selectivity to one of the products, viz. α-phenylethanol decreases, while the selectivity to the other product, viz. phenylacetaldehyde increased, which is probably due to the conversion of the former in to latter. Oxidation of α-phenylethanol to phenylacetaldehyde by tertiary butoxide may occur in this reaction, as formation of tertiary butoxide in the oxidation of alcohol with *tert*-butylhydroperoxide has been reported in the literature [37]. It is supported by increase in the selectivity of phenylacetaldehyde. The selectivity to acetophenone increases with increase in time since acetophenone is not a precursor of any daughter product. Similar to acetophenone the selectivity to benzaldehyde increases with time for both the feed ratios. The selectivity to α-phenylethanol and acetophenone at the end of 6 h, illustrates more rapid formation of α-phenylethanol than acetophenone. Hence, oxidation of the second carbon of the side chain is supported to be sterically retarded. The conversion and products selectivity over Mn-MCM-41 (Si/Mn = 56, 73 and 104) display nearly similar trend as that of Mn-MCM-41 (29). But the conversion over

these catalysts is less than Mn-MCM-41 (29). So this observation provides the order of the activity of catalysts Mn-MCM-41 (29) > Mn-MCM-41 (56) > Mn-MCM-41 (73) > Mn-MCM-41 (104). It is also the order of manganese content of the catalyst. Formation of the intermediate to yield acetophenone, α-phenylethanol, benzaldehyde and phenylacetaldehyde is illustrated in the following reaction scheme.

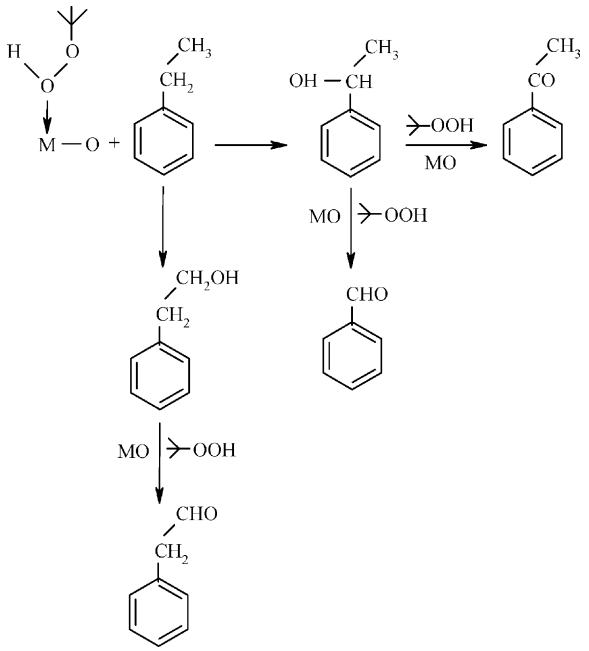

t-Butylhydroperoxide is activated by co-ordinating with metal oxide. The activated distant oxygen of co-ordinated *t*-butylhydroperoxide reacts with ethylbenzene to yield the above-mentioned products. α-Phenylethanol from ethylbenzene is produced by insertion of oxygen between carbon hydrogen bond of the methylene group. Abstraction of an alcoholic OH hydrogen and the CH hydrogen by the activated *t*-butylhydroperoxide oxygen yields acetophenone. Similar abstraction of OH hydrogen of α-phenylethanol by the activated *t*-butylhydroperoxide yields benzaldehyde by forming methane. Similar to formation of α-phenylethanol, the methyl group of ethylbenzene could also be acted upon by activated *t*-butylhydroperoxide to yield β-phenylethanol, which is to be very rapidly oxidized to phenylacetaldehyde. The rapid oxidation is evidenced through GC–MS analysis which indicates absence of 2-phenylethanol. So the main product obtained is found to be α-phenylethanol.

3.10. Selectivity of products

Formation of acetophenone requires chemisorption of alkyl hydroperoxide on the Lewis acid sites of the catalyst. Oxidation of the secondary carbon of ethylbenzene to α-phenylethanol, and appropriate cleavage of bonds give acetophenone. The selectivity to acetophenone is less in the beginning of the reaction (up to 6 h). The reaction is almost complete after about 24 h, when the TBHP efficiency reaches a maximum. After 24 h, no TBHP is detected in the reaction mixture. The results obtained over Mn-MCM-41 (56), Mn-MCM-41 (73) and Mn-MCM-41 (104) show similar trend for conversion and products selectivity. Although the conversion trend over these three catalysts is similar to that of Mn-MCM-41 (29), the magnitude is slightly less particularly for Mn-MCM-41 (104). The slight decrease is attributed to low content of manganese.

The increase in selectivity to benzaldehyde is observed with increase in time over all the catalysts. The observation suggests the influence of catalysts on the decomposition of α-phenylethanol to benzaldehyde. The selectivity to phenylacetaldehyde increases with increase in time. Since this product is produced from 2-phenylethanol, formation of the latter in the reaction can be expected. But GC analysis indicated absence of this product suggesting rapid conversion of it to 2-phenylacetaldehyde.

When the temperature is raised to 353 K similar trend for conversion and products selectivity is observed, and the results are presented in Table 4. The conversion increases with increase in time over all the catalysts. The selectivity to acetophenone increases as the temperature raises from 333 to 353 K but at 373 K a gradual decreases is observed, hence 353 K is the optimum temperature for the experiments.

3.11. Influence of the Si/Mn molar ratio

When the oxidation of ethylbenzene is carried out in the absence of catalyst, no significant conversion is observed. Negligible conversion of ethylbenzene is observed in the presence of MnO_2/SiO_2. The effect of Mn content in MCM-41 on the oxidation of ethylbenzene is presented in Tables 3 and 4. The conversion is high (Fig. 8) with increasing Mn-content in MCM-41 (example Si/Mn = 29). The selectivity to products is high over Mn-MCM-41 (29) but less over Mn-MCM-41 (104). This indicates that Mn is more uniformly dispersed and rich on the surface of the former than the latter. In all the cases, however, the product distribution shows that the oxidation of the secondary carbon is more predominant with formation acetophenone and α-phenylethanol.

3.12. Effect of temperature on oxidation

The effect of temperature on ethylbenzene conversion is studied at 333 and 353 K over Mn-MCM-41 (29) with feed ratios of EB: TBHP; 1:1 and 1:3. The results are presented in Tables 3 and 4. Conversion increases with time in both feed ratios. Selectivity to α-phenylethanol decreases with time while that of others increases with time. The similar results

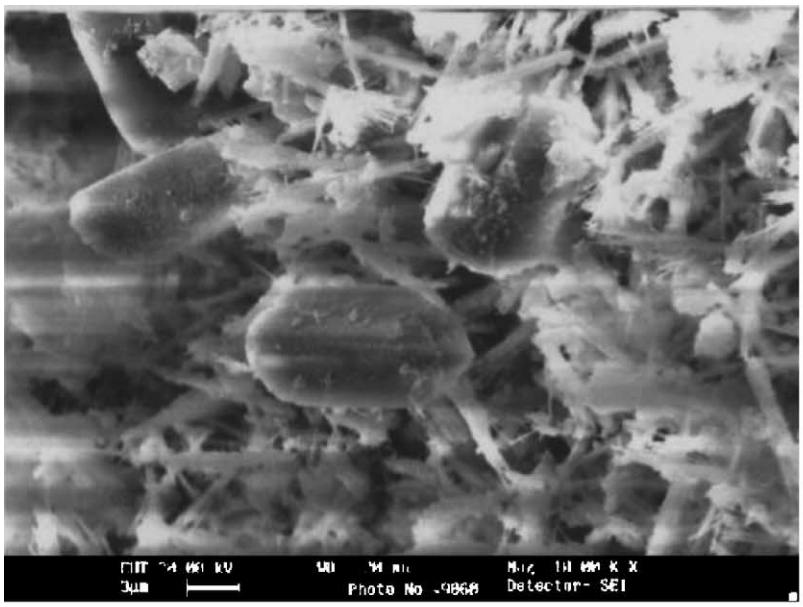

(a)

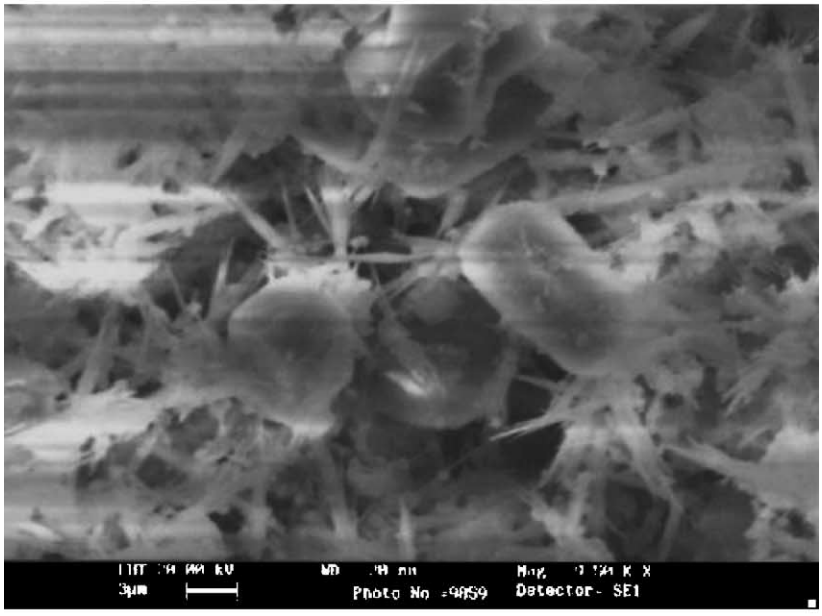

(b)

Fig. 7. SEM picture have: (a) Mn-MCM-41 (29); and (b) Mn-MCM-41(73).

are also obtained for all the catalysts (Tables 3 and 4). Comparison of conversion, over all the catalysts gives the order of activity of catalysts as Mn-MCM-41 (29) > Mn-MCM-41 (56) > Mn-MCM-41 (73) > Mn-MCM-41 (104), which is also the order of the active sites content namely manganese.

Comparison of results at 333 and 353 K illustrates more conversion and product selectivity for the latter than the former due to more activation of *t*-butylhydroperoxide at 353 K (Fig. 9). The reaction was also tested at 373 K with feed ratio of EB: TBHP; 1:1 and 1:3, but the conversion was found to be less, which might be attributed to the decomposition of *t*-butylhydroperoxide.

3.13. Effect of TBHP concentration

Comparison of the effect of feed ratio on conversion and products selectivity can be made from the data presented in the Tables 3 and 4. For example at 333 K when the feed ratio is changed from 1:1 to 1:3 increase in conversion is observed over Mn-MCM-41 (29). As the reaction depends on concentration of *t*-butylhydroperoxide activated by manganese,

Table 3
Oxidation of ethylbenzene at 333 K

Catalysts	Mole ratio	1:1				1:3			
	Time (h)	6	12	18	24	6	12	18	24
Si/Mn = 29	Conversion (wt.%)	29.1	44.4	51.3	58.5	37.4	47.8	55.0	64.9
	Selectivity (%)								
	α-Phenyl ethanol	81.5	61.7	45.4	32.8	85.3	71.2	53.1	36.4
	Acetophenone	16.9	23.9	31.3	38.4	14.7	20.3	33.1	40
	Benzaldehyde	1.1	4.5	8.1	12.9	0	3.3	6.7	12.4
	Phenyl acetaldehyde	0	4.8	9.5	11.4	0	5.2	7.1	11.2
	Others	0.5	5.1	5.7	4.5	0	0	0.1	0
Si/Mn = 56	Conversion (wt.%)	24.6	44.0	50.2	57.0	36.8	48.0	53.9	63.9
	Selectivity (%)								
	α-Phenyl ethanol	77.1	59.2	43.6	31.5	83.4	69.8	50.8	33.9
	Acetophenone	15.1	20.8	29.6	36.7	13.5	18.9	29.7	37.8
	Benzaldehyde	2.5	5.3	7.8	12.6	2.3	5.3	8.5	14.0
	Phenyl acetaldehyde	2.5	6.1	10.7	15.7	0.8	6	10.4	13.0
	Others	2.8	8.6	8.3	3.5	0	0	0.6	1.3
Si/Mn = 73	Conversion (wt.%)	19.8	40.0	47.0	52.8	34.2	44.9	49.4	59.2
	Selectivity (%)								
	α-Phenyl ethanol	74.3	58.4	45.0	30.1	80.0	65.2	47.2	32.0
	Acetophenone	14.2	19.9	27.7	36.1	13.0	20.1	27.8	35.6
	Benzaldehyde	4.5	8.4	11.8	15.7	4.0	6.5	9.8	16.7
	Phenyl acetaldehyde	4.0	7.5	10.9	17.6	3.0	8.2	12.0	15.0
	Others	3.0	5.8	4.6	1.1	0	0	3.2	0.7
Si/Mn = 104	Conversion (wt.%)	17.9	42.1	48.1	51.1	30.9	45.0	48.2	55.5
	Selectivity (%)								
	α-Phenyl ethanol	71.3	56.0	40.2	28.7	78.8	59.8	42.1	29.8
	Acetophenone	14.4	19.0	26.3	35.1	11.9	18.0	25.4	34.0
	Benzaldehyde	7.9	12.3	15.4	18.7	6.0	8.5	11.3	17.0
	Phenyl acetaldehyde	5.6	9.1	11.9	16.5	3.3	10.2	15.8	18.9
	Others	1.1	3.6	6.2	1.0	0	3.5	5.4	0.3

Reaction condition: 0.3 g of catalyst; temperature 333 K; flow rate of nitrogen 75 ml/h.

conversion with a feed ratio of 1:3 is more than that for 1:1. The selectivity to α-phenylethanol for the feed ratio 1:3 is more than that with 1:1 at every interval of time. The selectivity to acetophenone also shows a similar trend (Fig. 10) suggesting a rapid that the conversion of ethylbenzene to α-phenylethanol than its conversion to other products at the feed ratio of EB: TBHP; 1:3 than 1:1. Similar trend for conversion and products selectivity is also observed for other catalysts.

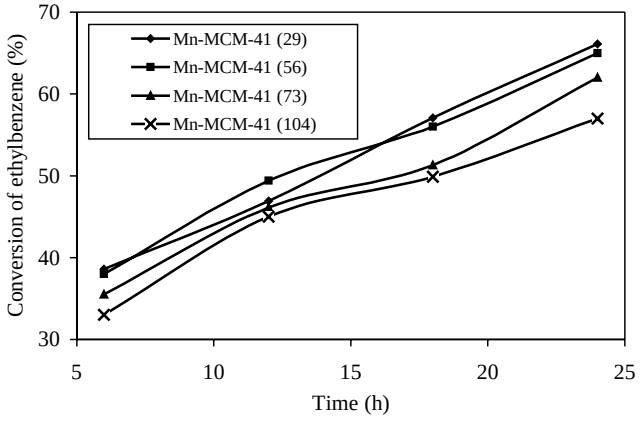

Fig. 8. Effect of temperature the conversion of ethylbenzene over Mn-MCM-41 (29), Mn-MCM-41 (56), Mn-MCM-41 (73) and Mn-MCM-41 (104) at 353 K (feed ratio 1:3).

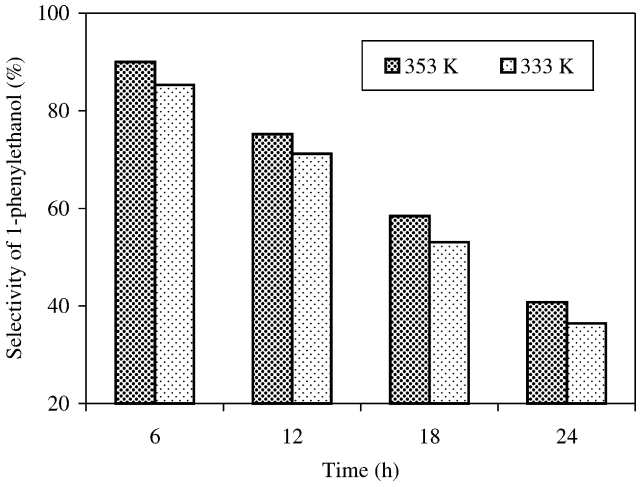

Fig. 9. Selectivity of α-phenylethanol over Mn-MCM-41 (29) at 333 and 353 K (feed ratio 1:3).

Table 4
Oxidation of ethylbenzene at 353 K

Catalysts	Mole ratio	1:1				1:3			
	Time (h)	6	12	18	24	6	12	18	24
Si/Mn=29	Conversion (wt.%)	34.3	46.8	50.9	60.5	38.6	46.9	57.1	66.1
	Selectivity (%)								
	α-Phenyl ethanol	83.5	65.8	48.1	36.1	90.0	75.2	58.4	40.8
	Acetophenone	14.0	25.4	32.0	39.0	10.0	21.5	35.8	43.8
	Benzaldehyde	0	3.0	7.1	10.8	0	1.5	3.0	5.1
	Phenyl acetaldehyde	2.5	5.8	10.5	13.4	0	1.8	2.8	10.3
	Others	0	0	2.3	0.7	0	0	0	0
Si/Mn=56	Conversion (wt.%)	32.1	45.7	47.0	59.0	38.0	49.4	56.0	65.0
	Selectivity (%)								
	α-Phenyl ethanol	80.1	62.5	45.1	33.8	86.1	73.5	54.9	38.8
	Acetophenone	13.1	22.8	27.4	34.5	12.2	22.2	33.4	40.2
	Benzaldehyde	2.8	4.5	7.8	12.0	0	2.8	5.3	8.5
	Phenyl acetaldehyde	4.0	8.0	15.6	19.0	1.0	1.5	6.0	12.1
	Others	0	2.2	4.1	0.7	0.7	0	6.4	0.4
Si/Mn=73	Conversion (wt.%)	30.9	41.0	49.3	61.8	35.5	46.1	51.3	62.0
	Selectivity (%)								
	α-Phenyl ethanol	77.2	60.4	43.8	29.5	84.0	68.1	50.1	36.9
	Acetophenone	11.9	20.0	25.0	31.9	14.0	25.2	31.0	36.9
	Benzaldehyde	4.5	7.0	9.5	16.8	1.0	3.0	6.5	10.2
	Phenyl acetaldehyde	6.4	10.3	17.0	19.3	1.0	3.7	8.1	13.0
	Others	0	2.3	4.7	2.5	0	0	4.4	3.0
Si/Mn=104	Conversion (wt.%)	28.9	39.9	46.5	55.9	33.0	45.0	49.9	57.0
	Selectivity (%)								
	α-Phenyl ethanol	73.5	58.4	42.0	28.1	80.9	66.3	47.8	33.8
	Acetophenone	10.0	17.1	22.9	25.3	15.3	23.2	29.8	31.5
	Benzaldehyde	6.7	8.2	10.5	18.0	2.0	5.1	7.6	12.0
	Phenyl acetaldehyde	8.5	12.0	18.0	20.6	1.8	4.5	10.0	15.3
	Others	1.3	4.2	6.6	8.0	0	0.9	4.8	7.4

Reaction condition: 0.3 g of catalyst; temperature 353 K; flow rate of nitrogen 75 ml/h.

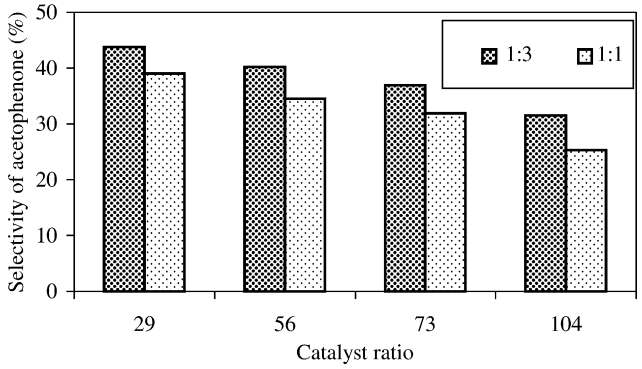

Fig. 10. Selectivity of acetophenone over Mn-MCM-41 (29); Mn-MCM-41 (56); Mn-MCM-41 (73) and Mn-MCM-41 (104) at 24 h (temperature 353 K).

4. Conclusion

Mn-MCM-41 has been synthesized hydrothermally with Si/Mn = 29, 56, 73 and 104. The presence of manganese in the framework is evident through ESR and DRS-UV analysis. The catalytic activity of Mn-MCM-41 has been examined for liquid phase oxidation of ethylbenzene using *t*-butylhydroperoxide as oxidant. At 333 and 353 K, the study indicates high activity for all the catalysts. Both primary and secondary carbons of the side chain of ethylbenzene are observed to be acted upon by activated *t*-butylhydroperoxide. α-Phenylethanol is observed as the major product. The other products obtained are acetophenone, benzaldehyde and phenylacetaldehyde. So this study reveals that Mn-MCM-41 can be a convenient ecofriendly substitute for hazardous stoichiometric oxidants.

References

[1] M. Rogovin, R. Neumann, J. Mol. Catal. A Chem. 138 (1999) 315.
[2] B. Notari, Stud. Surf. Sci. Catal. 37 (1987) 413.
[3] B. Notari, Stud. Surf. Sci. Catal. 60 (1991) 343.
[4] J.S. Reddy, R. Kumar, P. Ratnasamy, Appl. Catal. 58 (1990) L1.
[5] P. Kumar, R. Kumar, B. Pandey, Syn. Lett. (1995) 289.
[6] K.R. Reddy, A.V. Ramaswamy, P. Ratnasamy, J. Catal. 143 (1993) 275.
[7] T. Sen, M. Chatterjee. S. Sivasankar, J. Chem. Soc., Chem. Commun. (1995) 207.
[8] A. Bhanumik, M.K. Dongare, R. Kumar, Micro. Mater. 5 (1995) 173.
[9] P. Ratnasamy, R. Kumar, Stud. Surf. Sci. Catal. 97 (1995) 501.

[10] R. Vetrivel, P.R. Hari Prasad Rao, A.V. Ramaswamy, Stud. Surf. Sci. Catal. 83 (1995) 109.
[11] T. Selvam, A.P. Singh, J. Chem. Soc., Chem. Common. (1995) 883.
[12] K.R. Reddy, A.V. Ramaswamy, P. Ratnasamy, J. Chem. Soc., Chem. Commun. (1992) 1613.
[13] N.K. Mal, V. Ramaswamy, S. Gonaphathy, A.V. Ramaswamy, Appl. Catal. 125 (1995) 223.
[14] J.D. Chen, R.A. Sheldon, J. Catal. 153 (1995) 1.
[15] J.D. Chen, H.E.B. Lempers, R.A. Sheldon, J. Chem. Soc., Faraday Trans. 92 (1996) 1807.
[16] J.D. Chen, M.J. Haanepen, J.H.C. van Hooff, R.A. Sheldon, Stud. Surf. Sci. Catal. 84 (1994) 973.
[17] S. Menage, J.M. Vincent, C. Lambeaux, G. Chottard, A. Grand, M. Fontecave, Inorg. Chem. 32 (1993) 4766.
[18] R.H. Fish, K.J. Oberhausen, S. Chen, J.F. Richardson, W. Pierce, R.M. Buchanan, Catal. Lett. 18 (1993) 357.
[19] S. Menage, J.M. Vincent, C. Lambeaux, M. Fontecave, J. Chem. Soc., Dalton Trans. (1994) 2081.
[20] N. Kitajima, M. Ito, H. Fukui, Y. Moro-oka, J. Chem. Soc., Chem. Commun. (1991) 102.
[21] D. Tetrad, A. Rabion, J.B. Verlhac, J. Guilhem, J. Chem. Soc., Chem. Commun. (1995) 531.
[22] S. Menage, M.N. Collomb-Dunand-Sauthier, C. Lambeaux, M. Fontecave, J. Chem. Soc., Chem. Commun. (1994) 1885.
[23] J.M. Vincent, S. Menage, C. Lambeaux, M. Fontecave, Tetrahedron Lett. 35 (1994) 6287.
[24] R.H. Fish, R.H. Fong, K.J. Oberhausen, M.S. Konings, M.C. Vega, G. Christou, J.B. Vincent, R.M. Buchanan, N. J. Chem. 16 (1992) 727.
[25] C.M. Che, W.T. Tang, K.Y. Wong, W.T. Wong, T.F. Lai, J. Chem. Res. (S) (1991) 30.
[26] R. Burch, N.A. Cruise, D. Gleeson, S.C. Tsang, J. Chem. Soc., Chem. Commun. (1996) 951.
[27] R. Burch, N.A. Cruise, D. Gleeson, S.C. Tsang, J. Mater. Chem. 8 (1998) 227.
[28] R. Raja, J.M. Thomas, J. Chem. Soc., Chem. Commun. (1998) 1841.
[29] W.A. Carvalho, P.R. Varaldo, M. Wallau, U. Schuchardt, Zeolites 18 (1997) 408.
[30] Z.-R. Tian, W. Tong, J.-Y. Wang, N.-G. Duan, V.V. Krishnan, S.L. Suib, Science 276 (1997) 926.
[31] R. Schmidt, D. Akporiage, M. Stocker, O.H. Ellestad, J. Chem. Soc., Chem. Commun. (1994) 1493.
[32] A.V. Kiseler, V.I. Lygin, Infrared Spectra of Surface Compounds and Adsorbed Substances, Nauka, Moscow, 1992 (in Russian).
[33] K.A. Koyano, T. Tatsumi, J. Chem. Soc., Chem. Commun. (1996) 145.
[34] C.Y. Chen, H.X. Li, M.E. Davis, Micro. Mater. 2 (1993) 17.
[35] Z. Levi, A.M. Raitsimring, D. Goldfarb, J. Phys. Chem. 95 (1991) 7831.
[36] H.B.S. Chan, P.M. Budd, T. de V. Naylor, J. Mater. Chem. 11 (2001) 951.
[37] M. Fujiwara, Q. Xu, Y. Souma, T. Kobayashi, J. Mol. Catal. A Chem. 142 (1999) 77.